

A measurement at the first acoustic peak of the CMB with the 33 GHz interferometer

D.L. Harrison¹, J. A. Rubiño-Martin², S.J. Melhuish¹, R.A. Watson¹,
 R.D. Davies¹, R. Rebolo^{2,3}, R.J. Davis¹, C. M. Gutiérrez², J. F. Macias-Perez¹

¹University of Manchester, Jodrell Bank Observatory, Macclesfield, Cheshire SK11 9DL, UK

²Instituto de Astrofísica de Canarias, 38200 La Laguna, Tenerife, Canary Islands, Spain

³Consejo Superior de Investigaciones Científicas, Spain.

26 October 2018

ABSTRACT

This paper presents the results from the Jodrell Bank – IAC two-element 33 GHz interferometer operated with an element separation of 32.9 wavelengths and hence sensitive to 1° -scale structure on the sky. The level of CMB fluctuations, assuming a flat CMB spatial power spectrum over the range of multipoles $\ell = 208 \pm 18$, was found using a likelihood analysis to be $\Delta T_\ell = 63^{+7}_{-6} \mu\text{K}$ at the 68% confidence limit, after the subtraction of the contribution of monitored point sources. Other possible foreground contributions have been assessed and are expected to have negligible impact on this result.

Key words: cosmology: cosmic microwave background – cosmology: observations – large-scale structure of the Universe – instrumentation: interferometers.

1 INTRODUCTION

Observations of the angular power spectrum of the CMB temperature fluctuations are a powerful probe of the fundamental parameters of our universe. The amplitude and spatial distribution of these fluctuations can discriminate between competing cosmological models. Most inflationary models predict more power on scales of 0°.2 – 2°, in the form of a series of peaks. These are due to acoustic oscillations in the photon-baryon fluid, which are frozen into the CMB at recombination, with the peaks corresponding to regions of maximum compression and troughs regions of maximum rarefaction. Hence, the position of the first acoustic peak is a strong test for the geometry of the universe, since it corresponds to a fixed physical scale at the time of recombination projected onto the sky.

The previous result from the Jodrell Bank – IAC 33 GHz interferometer of $\Delta T_\ell = 43^{+13}_{-12} \mu\text{K}$, reported in Dicker et al. (1999), corresponds to an angular spherical harmonic $\ell \sim 110$, equivalent to $\sim 2^\circ$ structure. To investigate smaller angular scales the baseline was doubled; in this paper we analyze the data from this wide spacing configuration which corresponds to an angular spherical harmonic $\ell \sim 210$. The data presented here were taken at the Teide Observatory, Tenerife, between 27 May 1998 and 9 March 1999. The paper is organised as follows. The instrumental configuration is summarised in Section 2; a full description can be found in Melhuish et al. (1999). The basic data pro-

cessing is outlined in Section 3; for a more complete discussion see Dicker et al. (1999). The calibration method is also discussed in Section 3 and the data analysis in Section 4. A derivation of the fluctuation amplitude, after an estimate of the contribution of possible foregrounds, is given in Section 5.

2 THE 33 GHZ INTERFEROMETER

The interferometer consists of two horn-reflector antennas positioned to form a single E–W baseline, which has two possible lengths depending on the separation of the horns. The narrow spacing configuration has a baseline of 152 mm while in its wide spacing configuration the horns are 304 mm apart. For the observations presented here, the baseline was 304 mm. Observations were made at a fixed declination of Dec=+41°, using the rotation of the Earth to “scan” 24^h in RA each day. This “scan” runs through some of the lowest background levels of synchrotron, dust and free-free emission. The horn polarization is horizontal – parallel with the scan direction. There are two data outputs representing the cosine and the sine components of the complex interferometer visibility. The operating bandwidth covers 31 – 34 GHz, near a local minimum in the atmospheric emission spectrum; the antenna spacing corresponds to 32.9 wavelengths. The low level of precipitable water vapour, which is typically around 3 mm at Teide Observatory, permits the collection

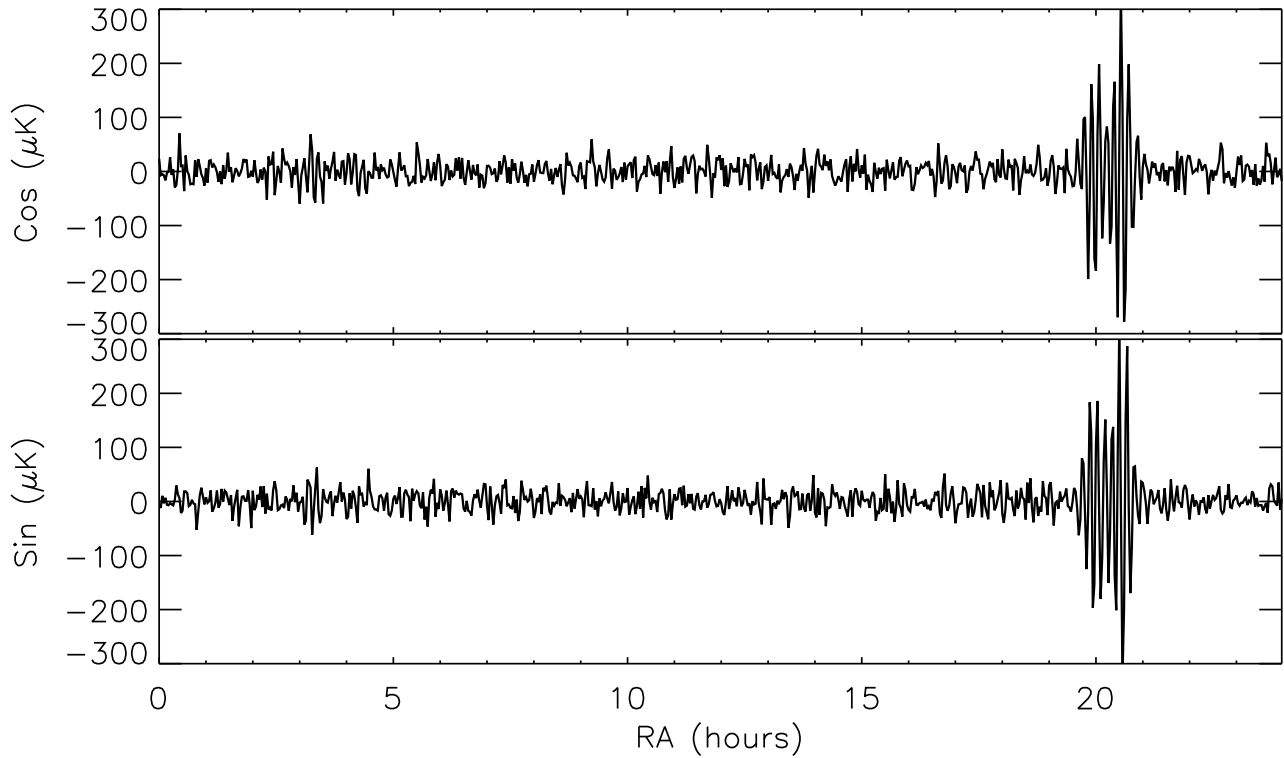


Figure 1. The total data stack, in 0.5° -bins, at Dec $+41^\circ$ collected over the period 27 May 1998 to 9 March 1999 and showing the cosine and sine visibility data. The number of days' observations included at each RA is between 180 – 210 days due to the removal of the Sun during the year. The Galactic plane crossing at the anti-centre is clearly visible at 21^h together with Cyg A at $20^\text{h}30^\text{m}$ and 3C84 at $3^\text{h}20^\text{m}$

of high quality data. Only 16 per cent of the data have been rejected, due to bad weather and the daily Sun transit.

The measured response of the interferometer is well approximated by a Gaussian with sigmas of $\sigma_{\text{RA}} = 2.25 \pm 0.03$ (in RA) and $\sigma_{\text{Dec}} = 1.00 \pm 0.02$ (in Dec), modulated by fringes with a period of $f = 1.74 \pm 0.02$ in RA. This defines the range of sensitivity to the different multipoles ℓ of the CMB power spectrum (C_ℓ) in the range corresponding to a maximum sensitivity at $\ell = 208$ (0.8°) and half sensitivity at $\Delta\ell = \pm 18$.

A known calibration signal (CAL) is periodically injected into the waveguide after the horns allowing a continuous calibration and concomitant corrections for drifts in the system gain and phase offset.

3 BASIC DATA PROCESSING AND CALIBRATION

The first step in the analysis is the removal of any variable baseline offsets from the data and the correction of a small departure from quadrature between the cosine and sine data. The data are calibrated relative to the CAL signal and re-binned into 2 - minute bins to ensure alignment in RA between successive scans. The data affected by the Sun and bad weather are removed and individual scans are weighted, with respect to their RMS error, to form a “stack”. The total stack of all the data used for this analysis is shown in

Fig. 1. The number of observations at each RA varies from 210 to 180 days due the removal of $\pm 0.5^\text{h}$ about the Sun transit each day.

The data are calibrated relative to CAL, although CAL itself needs to be calibrated by an astronomical source. The large size of the primary beam results in a reduced sensitivity to point sources and many days of observation are required to achieve a signal - to - noise ratio sufficient for calibration purposes. Consequently, the Moon is used as the primary calibrator as the power received from a single Moon transit is large enough to give signal - to - noise ratios of ~ 6000 .

The Moon was modelled as a uniform disk of radius r_{Moon} and a 33 GHz brightness temperature, T_b given by:

$$T_b = 202 + 27 \cos(\phi - \epsilon) \text{ K} \quad (1)$$

where ϕ is the phase of the Moon (measured from full Moon) and $\epsilon = 41^\circ$ is a phase offset caused by the finite thermal conductivity of the Moon (Gorenstein & Smoot 1981). It is sufficient to model the Moon as a uniform disk when correcting for its partial resolution by the interferometer. The effect of temperature variations across the Moon are negligible when compared to the error, 5.5 per cent, of the Gorenstein and Smoot model for the Moon's brightness temperature. The expected antenna temperature, T_E , can then be found by integrating over the disk of the Moon, multiplied by the normalized interferometer beam function:

$$T_E = \frac{T_b}{2\pi\sigma_{RA}\sigma_{Dec}} \times \int_0^{2\pi} \int_0^{r_{Moon}} \exp\left(-\frac{x^2}{2\sigma_{RA}^2} - \frac{y^2}{2\sigma_{Dec}^2}\right) \cos\left(\frac{2\pi x}{f}\right) d\Omega \quad (2)$$

where $x = r \cos \psi$ and $y = r \sin \psi$. σ_{RA} and σ_{Dec} are the RA and Dec beam sigmas (dispersion) and f is the fringe spacing.

Regular observations of the Moon were made; for each observation, equation 2 was evaluated numerically and an amplitude for CAL found such that the amplitude of the Moon in the processed data was equal to the predicted value. Using 27 observations of the Moon, an average amplitude for CAL of 14.7 ± 0.8 K was found. The error consists of a 1.4 per cent error in the measurements and an estimated 5.5 per cent in the moon model (Gorenstein & Smoot 1981). Fig. 2 shows our observations and how the measured brightness temperatures of the Moon change with phase.

The moon model used in this paper differs from the model given in Dicker et al. (1999). This data together with the addition data taken in the narrow spacing, section 6, will be the subject of a forthcoming paper, using the Moon model given in this paper.

4 LIKELIHOOD ANALYSIS

4.1 Theory

The temperature anisotropies of the CMB fluctuations are described by a two dimensional random field on the sky, the properties of which can be determined from the two point correlation function $C^{\text{CMB}}(\theta_{ij})$, where θ_{ij} is the angular separation of the two points.

$$C^{\text{CMB}}(\theta_{ij}) \equiv \left\langle \left(\frac{\Delta T_i}{T} \right) \left(\frac{\Delta T_j}{T} \right) \right\rangle \quad (3)$$

which can be expanded in terms of spherical harmonics as:

$$C^{\text{CMB}}(\theta_{ij}) = \sum_2^{\infty} \frac{(2\ell+1)}{4\pi} C_{\ell} P_{\ell}(\cos(\theta_{ij})) \quad (4)$$

In our analysis the form of the likelihood function is given by :

$$L \propto \frac{1}{|C|^{\frac{1}{2}}} \exp\left(-\frac{1}{2} D^T C^{-1} D\right) \quad (5)$$

where D is the data set and C is the covariance matrix, which represents the model of the CMB sky modulated by our observing strategy. The covariance matrix is composed of two terms, $C = S + N$ where S is the signal and N is the noise correlation matrix. The signal is the convolution of the two point correlation function and the auto-correlation function of the primary beam function of the interferometer.

$$S_{ij} = C^{\text{CMB}}(\theta_{ij}) \otimes S^{\text{beam}}(\theta_{ij}) \quad (6)$$

Using the band-power approximation where $\Delta T_{\ell} \equiv \sqrt{\ell(\ell+1)C_{\ell}/2\pi}$ * is assumed to be constant across the range of ℓ covered by the window function.

* There is a typographical error in Dicker et al. (1999), in the denominator the 8π should be 2π as written here.

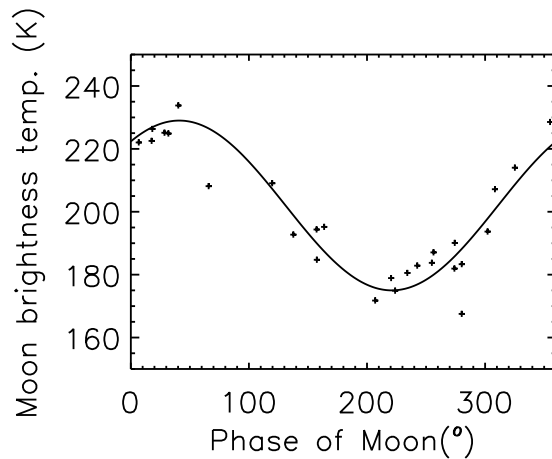


Figure 2. Measured value of the Moon's brightness temperature as a function of phase. Phase is measured from the full Moon. The solid line is the prediction of the model given by Gorenstein & Smoot (1981): $T_b = 202 + 27 \cos(\phi - \epsilon)$ in Kelvin. Each observation has been calibrated using $\text{CAL} = 14.7$ K.

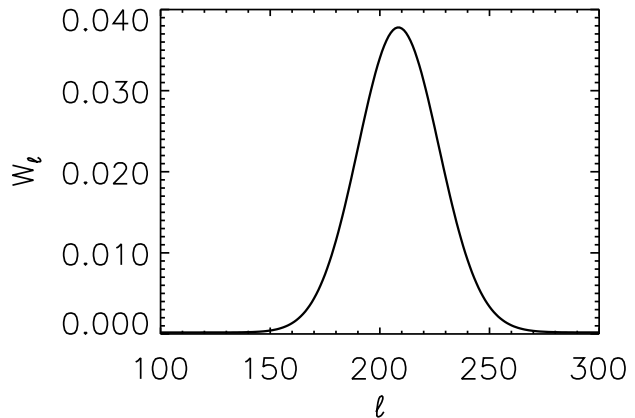


Figure 3. The window function of the interferometer in its wide-spacing configuration (304 mm ~ 32.9 wavelengths) which is well fit by $W_{\ell}(0) = 0.037 \times \exp\left(-\frac{(\ell-208)(\ell-209)}{694}\right)$

$$C^{\text{CMB}}(\theta_{ij}) = \frac{1}{2} (\Delta T)^2 \sum_2^{\ell_{\text{max}}} \frac{(2\ell+1)}{\ell(\ell+1)} P_{\ell}(\cos(\theta_{ij})) \quad (7)$$

where ℓ_{max} is the limit of the summation.

The sensitivity at an individual value of ℓ is given by the window function of the interferometer in Fig. 3. The window function was computed using the method of Muciaccia, Natioli & Vittorio (1997) to decompose the beam into spherical harmonics. The resulting function can be modelled by:

$$W_{\ell}(0) = 0.0377 \times \exp\left(-\frac{(\ell-208)(\ell-209)}{694}\right) \quad (8)$$

$W_{\ell}(0)$ falls to half power at $\ell = 208 \pm 18$.

The covariance matrix can now be calculated, by numerically evaluating equations (6) and (7). Equation (7) is

Table 1. Sources within a 4° -wide Dec strip centred on $+41^\circ$.

Name	RA ₂₀₀₀	Dec ₂₀₀₀	Mean Flux (Jy)
3C 84	03 ^h 19 ^m 48 ^s	+41 [°] 30' 42"	11.8
DA 193	05 ^h 55 ^m 31 ^s	+39 [°] 48' 49"	-
4C 39.25	09 ^h 27 ^m 03 ^s	+39 [°] 02' 21"	9.5
3C 345	16 ^h 42 ^m 59 ^s	+39 [°] 48' 37"	9.0
BL Lac	22 ^h 02 ^m 43 ^s	+42 [°] 16' 40"	3.7

evaluated to $\ell_{max} = 300$, where the sensitivity of the interferometer, $W_\ell(0)$, is negligible. The result of equation (7), $C_{ij}^{CMB}(\theta_{ij})$, is used to calculate the required value of S_{ij} using equation (6). The covariance of two points with an angular separation of θ_{ij} is then given by $C_{ij} = S_{ij} + N_{ij}$.

4.2 The results and the Galactic Cut

Any analysis should take account of likely Galactic emission. At Dec $+41^\circ$ the ranges $21^\circ 48' - 3^\circ 48'$ RA and $6^\circ 12' - 19^\circ 30'$ RA are at Galactic latitude $b \geq 10^\circ$. To find regions free of significant Galactic emission, 48 intervals of 5 hours in RA were analysed as described above, stepping every 0.5 hours. It was found that the above cut was in general agreement with the higher latitude results, except the region $2^\circ 48' - 3^\circ 48'$ which was excluded; this is due to the Galactic plane emission and difficulties in subtracting the contribution of 3C84, see Section 5.1.

The likelihood analysis of the ranges $21^\circ 48' - 2^\circ 48'$ RA and $6^\circ 12' - 19^\circ 30'$ RA gives $\Delta T = 78.5^{+12.5}_{-12.0} \mu K$ and $\Delta T = 69.5^{+12.5}_{-12.0} \mu K$ for the cosine channel and the sine channel respectively. The likelihood analysis using both channels simultaneously gives $\Delta T = 70.0^{+7.0}_{-6.5} \mu K$ at the 68 percent confidence level.

5 THE EFFECT OF FOREGROUNDS ON THE RESULTS

5.1 Point Sources

The 5 strongest sources with $S(33 \text{ GHz}) \geq 2 \text{ Jy}$ within a 4° strip centred on Dec $+41^\circ$, listed in table 1, are routinely monitored by the University of Michigan at 4.8, 8.0 and 14.5 GHz and in the Metsahovi programme at 22.0 and 37.0 GHz. Using these data over the period of our observations, it was possible to assess their mean flux densities at 33 GHz. These were then convolved with the two-dimensional interferometer beam pattern centred on Dec $+41^\circ$ and converted to antenna temperatures using the factor $6.90 \mu K Jy^{-1}$; in this form these sources may be subtracted from the data.

The data ranges $21^\circ 48' - 2^\circ 48'$ RA and $6^\circ 12' - 19^\circ 30'$ RA were analyzed together, subtracting the point sources as discussed above. Each channel was analyzed independently and then combined for a joint analysis. For the cosine channel $\Delta T = 69.5^{+12.5}_{-11.5} \mu K$, for the sine channel $\Delta T = 62.5^{+13.0}_{-11.5} \mu K$ and combining both channels gives $\Delta T = 64.0^{+7.0}_{-6.0} \mu K$ at the 68 per cent confidence level and $\Delta T = 64.0^{+14.5}_{-13.0} \mu K$ at the 95 per cent confidence level. The likelihood curve of this analysis is shown in Figure 4.

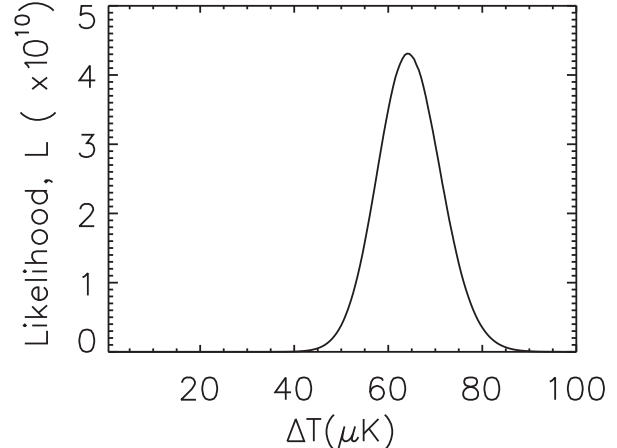


Figure 4. The likelihood curve of the joint analysis of both channels of the point source-subtracted data. $\Delta T = 64.0^{+7.0}_{-6.0} \mu K$ at the 68 per cent confidence level and $\Delta T = 64.0^{+14.5}_{-13.0} \mu K$ at the 95 per cent confidence level.

The contribution of unresolved point sources was estimated according to the results of Franceschini et al. (1989), at 33 GHz resolution of 0.8° this is expected to be $\sim 11 \mu K$, which adds in quadrature to the CMB signal. The contribution of unresolved sources then accounts for approximately $1 \mu K$ of the total signal and accordingly the best estimate of the intrinsic CMB fluctuation amplitude is $\Delta T = 63.0^{+7.0}_{-6.0} \mu K$ at $\ell = 208$.

5.2 Spinning Dust

de Oliveira-Costa et al. (1998) estimated the contribution of spinning dust in a 19 GHz map of 3° resolution by correlating it with the DIRBE sky maps, finding $\Delta T \sim 66 \pm 22 \mu K$. Using the IRAS 100 μK map, Gautier et al. (1992) investigated the spatial index of the dust, finding on scales between 8° and $4'$ that $\Delta T \propto \ell^{-3/2}$. This, combined with the expected spectral index of the spinning dust of $-3.3 < \beta_{\text{spin}} < -4$ (de Oliveira-Costa et al. 1998); allowed the estimation of the contribution of spinning dust at 33 GHz and 0.8° resolution. The expected signal in our data due to spinning dust was found to be $\Delta T^{\text{dust}} \approx 1.5 \pm 0.5 \mu K$. This again adds in quadrature to the total signal, therefore the contribution from spinning dust is expected to be negligible.

5.3 Diffuse Galactic Emission

An estimate of the amplitude of the diffuse Galactic component in our data can be computed using the results obtained in the same region of the sky by the Tenerife CMB experiments (Gutiérrez et al. 2000). At 10.4 GHz and on angular scales centred on $\ell = 20$ the maximum Galactic component was estimated to be $\leq 28 \mu K$. Assuming that this contribution is entirely due to free-free emission ($\beta = -2.1$) and a conservative Galactic spatial power spectrum of $\ell^{-2.5}$, the predicted maximum Galactic contamination in the data presented here is $0.8 \mu K$, less than 2 per cent of our measured value. Any such contribution would add in quadrature to

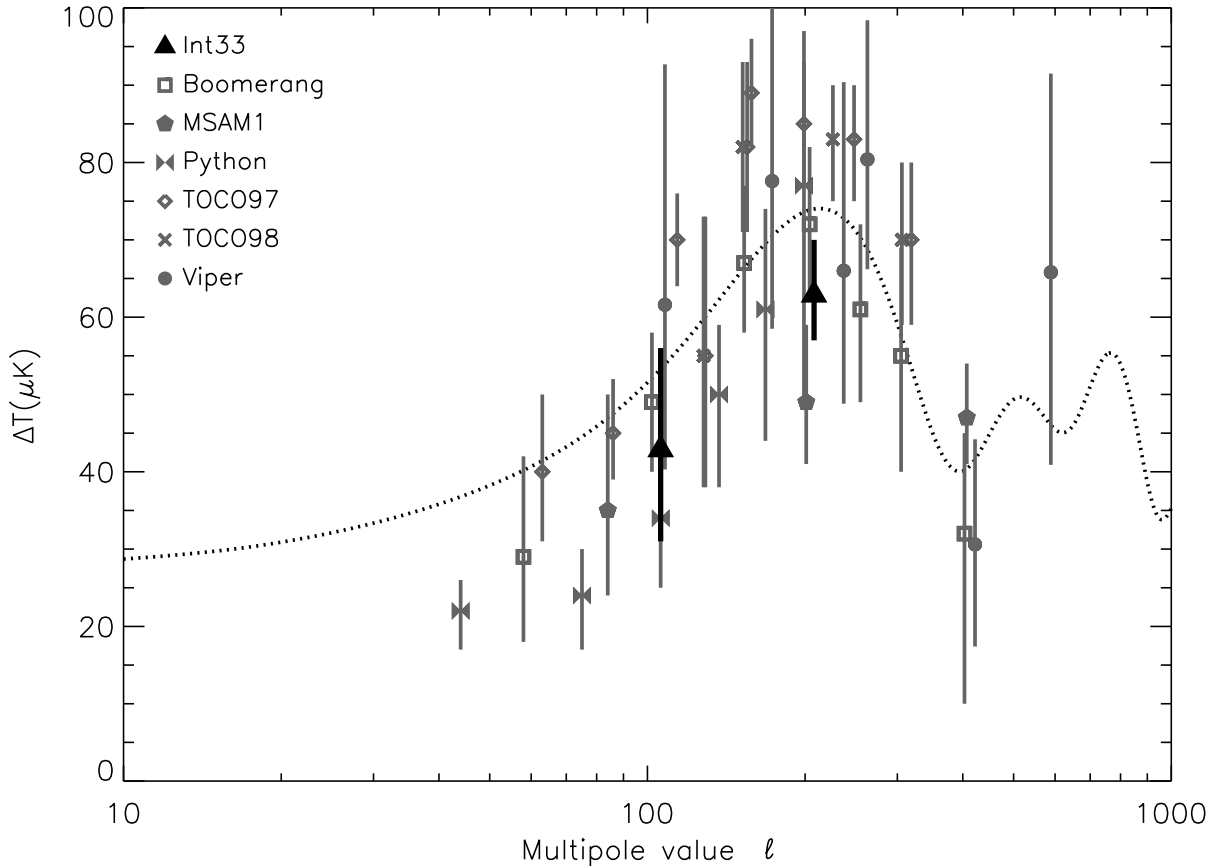


Figure 5. Values of ΔT published in the past year, as a function of ℓ . Our present result of $\Delta T_\ell = 63^{+7}_{-6} \mu\text{K}$ is shown by the heavy line at $\ell \sim 200$. The result of Dicker et al. (1999) is shown by the heavy line at $\ell \sim 100$. The dotted line represents the model given by $\Omega_b = 0.05$, $\Omega_{\text{CDM}} = 0.40$, $\Omega_\lambda = 0.55$ and $H_0 = 70 \text{ km s}^{-1} \text{ Mpc}^{-1}$; this is shown for illustrative purposes and does not represent a fit to the data.

Table 2. Values of ΔT around $\ell \sim 200$ published in the past year.

Experiment	Freq. (GHz)	ΔT (μK)	Multipole, ℓ	Reference
Int33	33	63^{+7}_{-6}	208^{+18}_{-18}	This Paper
MSAM1	156	49^{+10}_{-8}	201^{+70}_{-70}	Wilson et al. (2000)
Viper	40	$66^{+24.4}_{-17.2}$	237^{+111}_{-99}	Peterson et al. (2000)
Boomerang	150	72^{+10}_{-10}	204^{+28}_{-21}	Mauskopf et al. (1999)
Python V	41	77^{+20}_{-28}	199^{+15}_{-15}	Coble et al. (1999)
TOCO98	144	83^{+7}_{-8}	226^{+56}_{-37}	Miller et al. (1999)
TOCO97	35	85^{+8}_{-8}	199^{+29}_{-38}	Torbet et al. (1999)

that from the CMB, and so is insignificant. The true make-up of the 10.4 - GHz Galactic foreground emission will have a steeper average spectral index since synchrotron radiation with $\beta \sim -3$ will contribute to the measured value, therefore the contribution to our result will be even lower than stated.

6 CONCLUSIONS

In this paper we describe the results taken with the Jodrell Bank - IAC 33 GHz interferometer in its wide spacing con-

figuration, which is sensitive to structure at $\ell = 208 \pm 18$. In the final result of $\Delta T = 63.0^{+7.0}_{-6.0} \mu\text{K}$ possible foreground contributors have been considered, the most significant of which are point sources. In Section 5.1 the contribution of strong, monitored sources are removed from the data. To allow for the contribution of unresolved sources the lower limit on ΔT has been increased. In Sections 5.2 and 5.3, the contributions from dust and diffuse Galactic emission are found to be negligible. We believe our result represents the intrinsic CMB fluctuation signal at $\ell = 208 \pm 18$. The quoted error in our result is dominated by sample variance, result-

ing from the finite number of beam areas observed.

Table 2 and Fig. 5 show our result alongside others published in the last year from experiments covering similar angular scales. These experiments have been made at a range of different frequencies and regions of the sky. Our result is in good agreement with the published data around $\ell \sim 200$. The results at $\ell \sim 200$ appear to be converging on a value of $\Delta T = 60 - 70 \mu\text{K}$. However, over the wider- ℓ range of 50 – 300 discrepancies appear in the data sets significantly greater than the quoted errors. There appears to be evidence for unknown systematic effects and possible foreground contamination remaining in the data sets.

Our interferometer results show a rise in the amplitude of the power spectrum between $\ell \sim 100$ and $\ell \sim 200$. This is intrinsic to the CMB since the parameters of the interferometer system, particularly the calibration, remain the same except for the spacing. The data in Fig. 5, despite the discrepancies referred to above, are strongly indicative of a peak in the power spectrum at $\ell \sim 200$.

The interferometer is currently in its narrow spacing configuration ($\ell \sim 110$), observing declinations spaced by $1^\circ.2$ from Dec $+37.4$ to $+43.4$; these data will significantly reduce the sample variance of the result published by Dicker et al. (1999) to the order of 5 per cent.

7 ACKNOWLEDGEMENTS

This work has been supported by the European Community Science program contract SCI-ST920830, the Human Capital and Mobility contract CHRXCT920079 and the UK Particle Physics and Astronomy Research Council. This work has been partially supported by the Spanish DGES projects PB95-1132-C02-01 and PB98-0531-C02-02. DLH and JFMP acknowledge the receipt of a PPARC Postgraduate Studentship. We thank Dr.H.Teräranta for providing data on point sources at 22 and 37 GHz. This research has made use of data from the University of Michigan Radio Astronomy Observatory which is supported by funds from the University of Michigan.

REFERENCES

Davies R. D., Wilkinson A., 1998, in Bouchet F., Tran Thanh Van J., eds, 33rd Rencontre de Moriond, Fundamental Parameters in Cosmology, Editions Frontières, Gif-sur-Yvette

Coble K., PhD Thesis, University of Chicago, 1999, astro-ph /9911419

de Bernardis P., et al. 2000, Nature, 404, 955

de Oliveira-Costa A., Tegmark M., Page L.A., Boughn S.P., 1998, ApJ, 509, L9

Dicker S.R., et al. 1999, MNRAS, 309, 750

Franceschini A., Toffolatti L., Danese L., De Zotti G., 1989, ApJ, 344, 35

Gautier T.N., Boulanger F., Perault M., Puget J.L., 1992, AJ 103 1313

Gorenstein M.V., Smoot G.F., 1981, ApJ, 244, 361

Gutiérrez C. M., Rebolo R., Watson R. A., Davies R. D., Jones A. W., Lasenby A. N., 2000, ApJ, In press

Hanany S., et al. 2000, astro-ph / 0005123

Lasenby A.N., 1996, in Bouchet F., Tran Thanh Van J., eds, 31st Rencontre de Moriond, Microwave Background Anisotropies, Editions Frontières, Gif-sur-Yvette, astro-ph/9611214

Mauskopf P.D., et al. 1999, astro-ph / 9911444

Melhuish S. J., et al. 1999, MNRAS, 305, 399

Miller A.D., et al. 1999, ApJ, 524, L1

Muciaccia P.F., Natoli P., Vittorio N., 1997, ApJ, 488, L63

Peterson J.B., et al. 2000, ApJ, 532, 57

Torbet E., et al. 1999, ApJ, 521, L79

Wilson G.W., et al. 2000, ApJ, 532, 83

Note added in proof

Our result of $\Delta T = 63.0^{+7.0}_{-6.0} \mu\text{K}$ at $\ell = 208$ is competitive with the latest published results from the Boomerang experiment, which found an amplitude for the first peak of $\Delta T = 69 \pm 8 \mu\text{K}$ at $\ell = 197 \pm 6$, (de Bernardis et al. 2000) and the Maxima experiment, which found a peak at $\ell \approx 220$ of amplitude $\Delta T = 78 \pm 6 \mu\text{K}$, (Hanany et al. 2000).